Huntingtin facilitates dynein/dynactin-mediated vesicle transport

Juliane P. Caviston, Jennifer L. Ross, Sheila M. Antony, Mariko Tokito, and Erika L. F. Holzbaur*

Department of Physiology, University of Pennsylvania School of Medicine, Philadelphia, PA 19104

Edited by Thomas C. Südhof, University of Texas Southwestern Medical Center, Dallas, TX, and approved April 26, 2007 (received for review November 30, 2006)

Cytoplasmic dynein is a multisubunit microtubule motor complex that, together with its activator, dynactin, drives vesicular cargo toward the minus ends of microtubules. Huntingtin (Htt) is a vesicle-associated protein found in both neuronal and nonneuronal cells that is thought to be involved in vesicular transport. In this study, we demonstrate through yeast two-hybrid and affinity chromatography assays that Htt and dynein intermediate chain interact directly; endogenous Htt and dynein coimmunoprecipitate from mouse brain cytosol. Htt RNAi in HeLa cells results in Golgi disruption, similar to the effects of compromising dynein/dynactin function. *In vitro* studies reveal that Htt and dynein are both present on vesicles purified from mouse brain. Antibodies to Htt inhibited vesicular transport along microtubules, suggesting that Htt facilitates dynein-mediated vesicle motility. *In vivo* inhibition of dynein function results in a significant redistribution of Htt to the cell periphery, suggesting that dynein transports Htt-associated vesicles toward the cell center. Together these findings indicate that Htt binds to dynein and acts in a complex along with dynactin and Htt-associated protein-1 to facilitate vesicular transport.

microtubule motility | membrane trafficking | molecular motors | bidirectional motility | Huntington's disease

Cytoplasmic dynein is a minus end-directed microtubule motor protein responsible for the transport of vesicles and organelles toward the cell center. Dynactin is a dynein activator that binds to both dynein and the microtubule. The dynein/dynactin complex is essential for a diversity of cellular trafficking events, such as vesicular trafficking from the endoplasmic reticulum to the Golgi and lysosomal motility (1). Cytoplasmic dynein and dynactin associate with intracellular cargoes through multiple mechanisms (1). Here we describe a mechanism by which dynein targets vesicular cargo through a direct interaction with Huntingtin (Htt).

Although Htt is enriched in the brain, the protein is widely expressed in all tissues and is associated with both vesicles and microtubules (2–5). Inactivation of the mouse Htt gene (*Hdh*) results in embryonic lethality (6), indicating an essential role for Htt in early development. Polyglutamine expansion in mutant Htt causes Huntington's disease, a neurodegenerative disorder that primarily affects striatal neurons. Mutant Htt disrupts axonal transport in squid axoplasm (7), *Drosophila* (8), and mammals (9, 10), suggesting a role for the protein in vesicle transport. Htt interacts with various proteins implicated in trafficking (6, 11), including Htt-associated protein-1 (HAP1), which in turn interacts with both dynactin and kinesin (12–14). Here we show that Htt interacts directly with dynein and facilitates vesicle motility along microtubules, indicating that Htt could be a scaffold, integrating protein–protein interactions that lead to effective intracellular transport of vesicular cargo.

Results

To understand how dynein targets vesicular cargo, we conducted a yeast two-hybrid screen to identify dynein-interacting proteins. Full-length dynein intermediate chain (DIC) was used as bait to identify binding partners from a human brain cDNA library. A positive interaction was detected between full-length DIC and a library clone that encodes a 162-amino acid fragment from the N terminus of Htt (residues 536–698).

To further map the DIC binding site of Htt, four constructs (Htt1–Htt4) spanning the full length of Htt (Fig. 1*A*) were *in vitro*-translated and incubated with DIC beads. Htt2 (601–1,483) bound to DIC beads (Fig. 1*B*), but not control beads (data not shown), verifying the region of interaction identified by the yeast two-hybrid clone. In contrast, Htt1 (1–600), Htt3 (1,484–2,225), and Htt4 (2,226–3,144) did not bind to the DIC column. Together these assays identify Htt residues 600–698 as both necessary and sufficient for binding to DIC.

To determine which region of DIC interacts with Htt, we used the yeast two-hybrid system to assay binding between Htt 536–698 and a series of DIC truncation constructs spanning the residues 1–120, 120–283, 1–283, and 283–644 (Fig. 1*A*). Cells coexpressing Htt 536–698 and DIC 1–283 had the strongest signal, demonstrating that amino acids 1–283 of DIC are required for binding to Htt (Fig. 1*C*).

To test the specificity of the interaction between Htt and endogenous dynein, we loaded mouse brain cytosol onto a GST-Htt$^{536-698}$ affinity column. The bound fraction was shown to contain dynein (Fig. 2*A*). To assess whether the interaction between dynein and Htt depends on dynactin, we loaded FPLC-purified dynein, which lacks dynactin (15), onto the GST-Htt$^{536-698}$ affinity matrix. Again, dynein bound specifically to the Htt column, indicating that dynactin is not required to mediate the interaction between dynein and Htt (Fig. 2*B*).

The above experiments indicate that the binding of Htt to dynein is both direct and specific. To examine the physiological relevance of the interaction, an immunoprecipitation was performed with DIC antibody on mouse brain cytosol. Full-length endogenous Htt was coimmunoprecipitated with dynein, along with dynactin, kinesin, and HAP1 (Fig. 2*C*). In contrast, Htt did not precipitate with control beads. The coprecipitation of Htt and DIC indicates that the endogenous proteins interact, although not all of the Htt present in the cytosol bound to the beads, suggesting that the dynein–Htt interaction may be regulated *in vivo*.

We next performed immunocytochemistry on HeLa cells with antibodies to both Htt and DIC (Fig. 2*D*). Both Htt and DIC are visible as puncta distributed throughout the cytoplasm with

Author contributions: J.P.C., J.L.R., S.M.A., M.T., and E.L.F.H. designed research; J.P.C., J.L.R., S.M.A., M.T., and E.L.F.H. performed research; M.T. contributed new reagents/analytic tools; J.P.C., J.L.R., S.M.A., and E.L.F.H. analyzed data; and J.P.C. and E.L.F.H. wrote the paper.

The authors declare no conflict of interest.

This article is a PNAS Direct Submission.

Abbreviations: Htt, Huntingtin; HAP1, Htt-associated protein-1; DIC, dynein intermediate chain; WD, tryptophan-aspartate; HEAT, Htt, elongation factor 3, a subunit of protein phosphatase 2A, and TOR1; DHC, dynein heavy chain.

*To whom correspondence should be addressed. E-mail: holzbaur@mail.med.upenn.edu.

This article contains supporting information online at www.pnas.org/cgi/content/full/0610628104/DC1.

CELL BIOLOGY

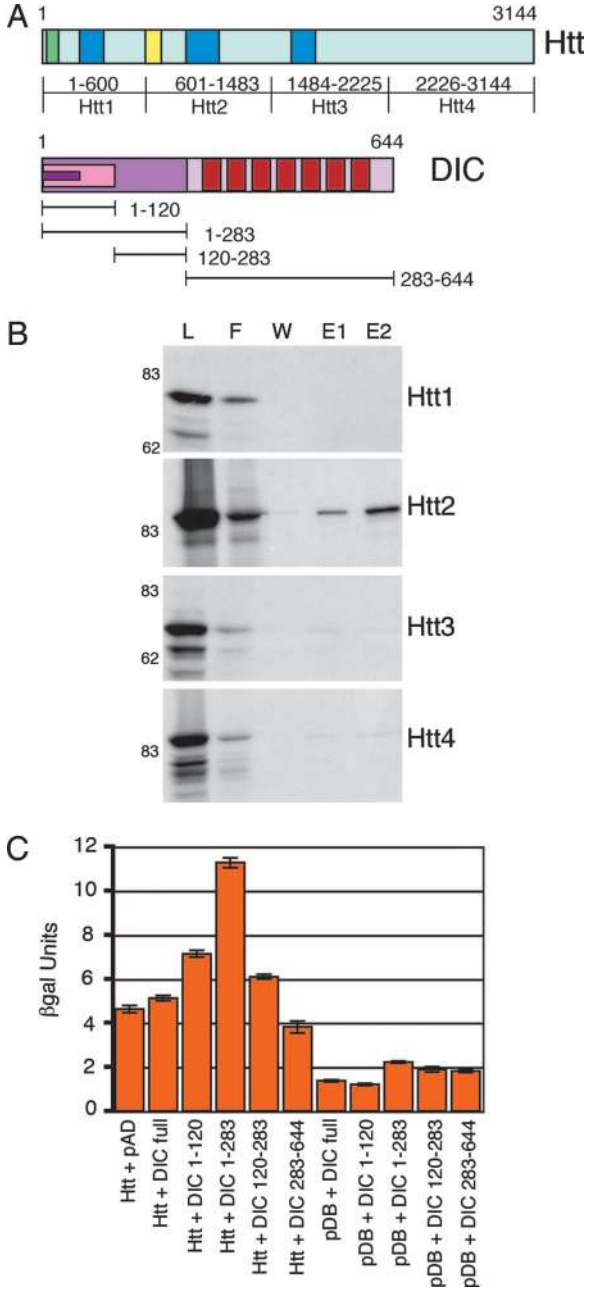

Fig. 1. Mapping the interaction between Htt and DIC. (*A*) (*Upper*) Htt has a polyglutamine region (green), HEAT repeat clusters (dark blue), and DIC interaction domain (yellow). (*Lower*) DIC has an N-terminal-coiled domain (magenta), dynactin interaction domain (pink), Htt interaction domain (purple), and seven WD repeats (red). (*B*) Four peptides (Htt1–Htt4) spanning the length of Htt were *in vitro*-translated, loaded on a DIC column, and eluted with 2 M NaCl. The lanes are load (L), flow-through (F), wash (W), elution 1 (E1), and elution 2 (E2). Only Htt2 was eluted from the DIC column. (*C*) Four DIC truncations (1–120, 1–283, 120–283, and 283–644) were tested for interactions with $Htt^{536-698}$ as assayed by β-galactosidase activity (SEM, $n = 3$). Controls include the activation domain (pAD) and DNA-binding domain (pDB) vectors.

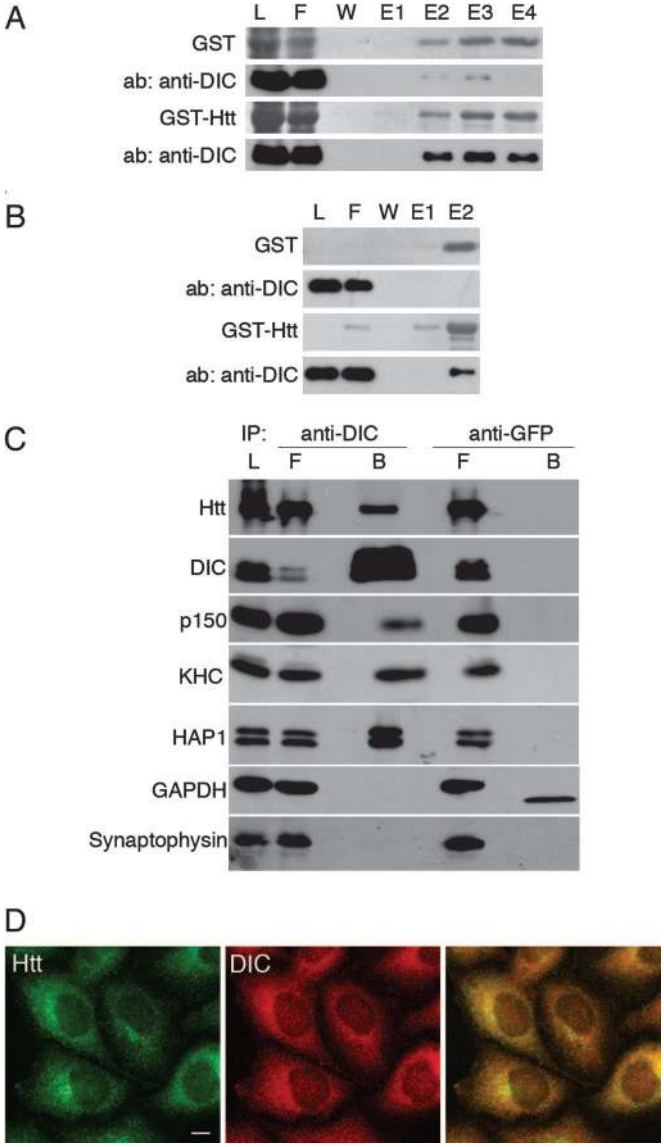

Fig. 2. Htt interacts with endogenous cytoplasmic dynein. (*A*) Affinity chromatography of GST beads (*Upper*) or GST-$Htt^{536-698}$ beads (*Lower*) incubated with mouse brain cytosol. SDS/PAGE gel samples from the load (L), flow-through (F), wash (W), and elutions (E1–E4) were stained to visualize GST or GST-Htt protein and then probed with a monoclonal anti-DIC antibody. DIC is present in fractions eluted with 20 μM glutathione from GST-Htt beads, but not from GST control beads. (*B*) Affinity chromatography of GST beads (*Upper*) or GST-Htt beads (*Lower*) incubated with FPLC-purified dynein derived from bovine brain. DIC is present in fraction E2 eluted from GST-Htt beads, but not from GST control beads. (*C*) Coimmunoprecipitation of endogenous Htt and DIC from mouse brain cytosol with a polyclonal antibody to DIC UP1467 (anti-DIC), but not a control antibody (anti-GFP). The load (L), flow-through (F), and bead (B) samples were probed with antibodies to Htt, DIC, dynactin (p150), kinesin heavy chain (KHC), and HAP1. Negative controls included GAPDH and synaptophysin. Blots probed for GAPDH showed some cross-reactivity with the GFP antibody light chain. (*D*) Htt and DIC have similar distributions in HeLa cells. Both Htt (green) and DIC (red) are distributed in tiny puncta throughout the cytoplasm, with overlapping concentrations at the Golgi in the perinuclear region (yellow). (Scale bar: 10 μm.)

concentrations at the Golgi, consistent with partial colocalization. Both Htt and DIC puncta align along the microtubules in HeLa and COS7 cells (data not shown).

We hypothesized that the association between Htt and DIC is involved in microtubule-based vesicular transport *in vivo*. To test our hypothesis, we used RNAi to specifically deplete either protein. The organization of the Golgi into tight stacks in the perinuclear region of the cell is dynein-dependent. Disruption of dynein by overexpression of the dynactin subunit dynamitin (p50) (16, 17), or depletion of either dynein (18) or dynactin (19), results in fragmentation of the Golgi. To confirm the Golgi

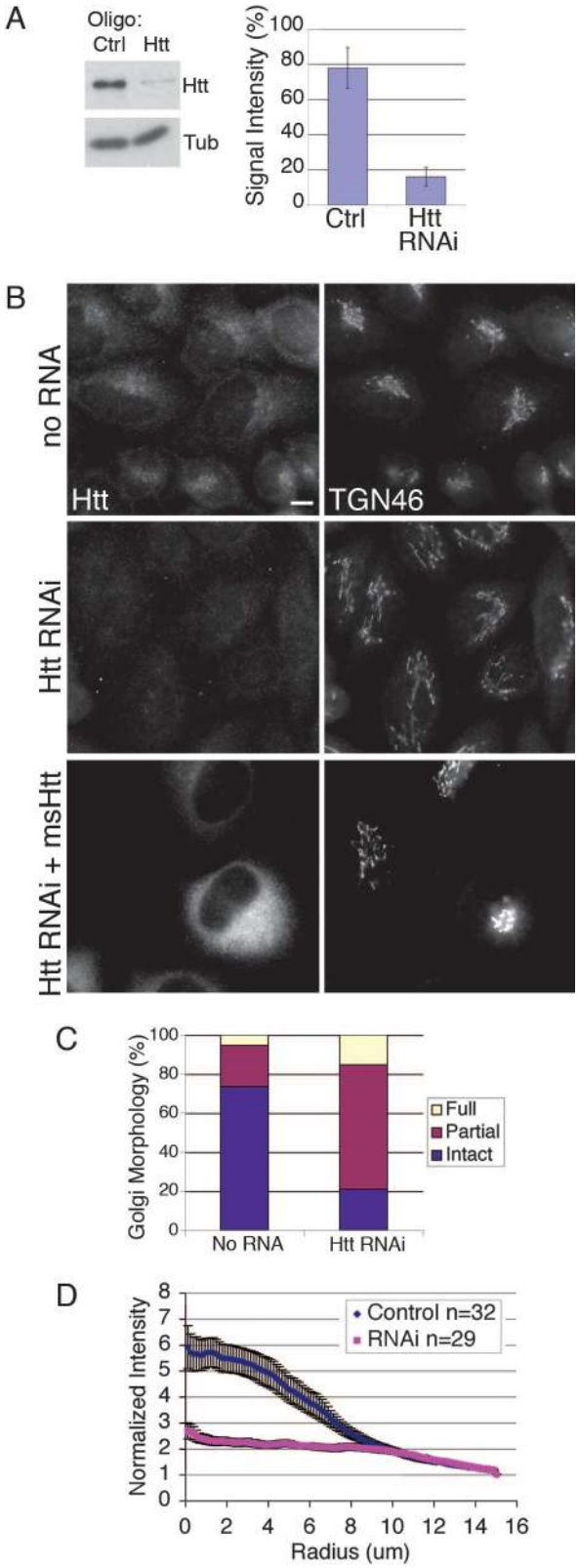

Fig. 3. Htt RNAi causes disruption of Golgi. (*A*) (*Left*) HeLa cells were treated with Htt RNAi or control oligonucleotides; cell extracts were blotted with antibodies to Htt and tubulin. (*Right*) Htt RNAi decreased Htt expression to 16 ± 5% of no RNA controls, whereas negative control oligonucleotides only modestly decreased expression (SEM, $n = 5$). (*B*) (*Top*) No RNA control cells immunostained for Htt and TGN46 have a normal Golgi. (*Middle*) Htt immunostaining is absent in Htt RNAi cells and the Golgi is disorganized, with tubules stretched out into the cytoplasm. (*Bottom*) Htt RNAi cells were transfected with plasmid DNA encoding mouse Htt. The transfected cell in the field has a much brighter Htt signal than nontransfected cells, and Golgi disruption is rescued. (Scale bar: 10 μm.) (*C*) Golgi morphology in Htt RNAi and no RNA control cells immunostained for TGN46 was qualitatively assessed and binned into three categories: intact, partial (tubulated), and full disruption (vesicular) (SEM, $n = 300$). (*D*) Images of Htt RNAi (SEM, $n = 29$) and no RNA control cells (SEM, $n = 32$) immunostained for TGN46 were analyzed with a radial profiling algorithm that measured the signal intensity for a series of 110 concentric circles (normalized by dividing by the area) emanating from the center of each cell. Control cells (blue) had a normal Golgi morphology, and signal was concentrated near the cell center. In contrast, in Htt RNAi cells (pink), the TGN46 signal was delocalized from the cell center.

disruption phenotype in our model system, we depleted dynein by RNAi of dynein heavy chain (DHC), which is encoded by a single gene. Interestingly, we observed that a 92 ± 2% reduction of DHC by RNAi also resulted in a 97 ± 1% inhibition of DIC expression (SEM, $n = 5$), indicating that a coregulatory mechanism governs the expression of these two subunits of dynein [supporting information (SI) Fig. 6]. As expected, RNAi of dynein in HeLa cells resulted in a dramatic fragmentation of the Golgi (SI Fig. 6*B*), with 98 ± 1% of cells displaying a fully dispersed Golgi (SEM, $n = 300$) (SI Fig. 6*C*).

We next investigated the effects of depleting Htt by RNAi and found that Htt knockdown results in partial Golgi disruption, suggesting that Htt and dynein may function in a similar pathway. In cells where Htt protein expression was reduced by 83 ± 5% compared to negative control levels (SEM, $n = 5$) (Fig. 3*A*), the Golgi appeared to be stretched out of its normally tightly organized stacks (Fig. 3*B*) or otherwise completely vesicular as observed in DHC RNAi cells. Further, 64 ± 4% of cells had a partially dispersed Golgi, compared to 21 ± 1% of no RNA control cells; and 15 ± 4% of Htt RNAi cells had a fully disrupted Golgi, compared to only 5 ± 1% of control cells (SEM, $n = 300$) (Fig. 3*C*). Immunostaining with another Golgi marker, GM130, showed similar results (data not shown.) The Htt knockdown results in less dramatic Golgi disruption than the DHC RNAi results, consistent with the observation that only a portion of Htt is associating with dynein at steady state. Quantitative analysis of Golgi elements in Htt RNAi cells shows that the Golgi becomes significantly less centrally localized and more tubulovesicular (Fig. 3*D*). The disrupted Golgi phenotype was rescued by transfection of mouse Htt plasmid DNA into Htt RNAi cells (Fig. 3*B* and SI Fig. 7), indicating the specificity of the effect of Htt depletion on Golgi morphology.

To further test our hypothesis that Htt participates in dynein-mediated vesicular transport, we conducted *in vitro* motility assays. Htt is known to be vesicle-associated (2), and, indeed, it was present along with dynein and dynactin in the vesicular fraction prepared from mouse brain cytosol (Fig. 4*A*). Vesicles purified from transgenic mice expressing low levels of p50-GFP incorporate stoichiometric amounts of the tagged subunit into the dynactin complex (20). The stable association of GFP-labeled dynactin with purified vesicles allows the visualization of dynein-based vesicular movement along microtubules by using total internal reflection microscopy.

When vesicles were preincubated with antibodies raised against Htt, the vesicles mostly dissociated from microtubules, in contrast to vesicles preincubated with control antibody (anti-Myc), which induced no significant change in microtubule association (Fig. 4*B*). In addition, the motility of the vesicles that did bind to microtubules in the presence of anti-Htt antibodies was significantly inhibited (Fig. 4*C*), and the inhibition was bidirectional (Fig. 4*D*), which is consistent with previous observations of decreased organelle motility with disruption of dynein/dynactin function (21). The inhibition of vesicular transport

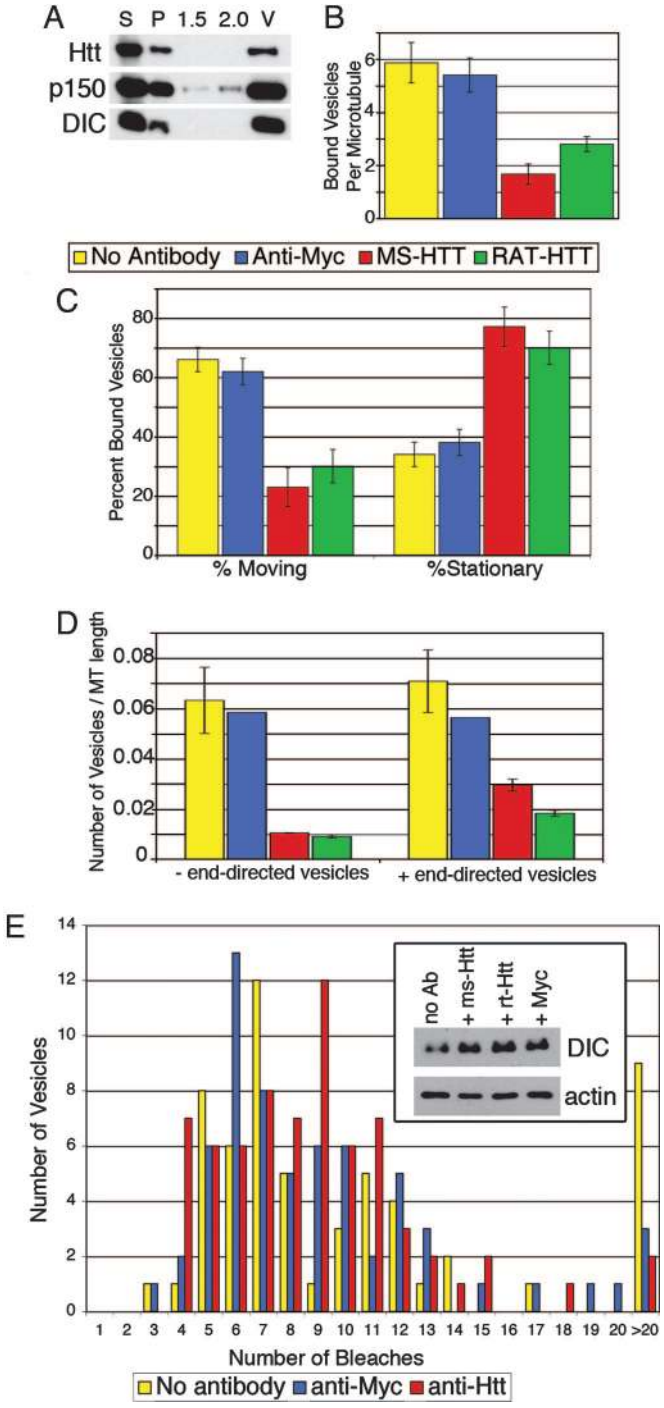

Fig. 4. Functional Htt is required for dynein-mediated vesicle transport *in vitro*. (*A*) Htt copurifies in the vesicle fraction with dynein and dynactin. Vesicles purified from p50-GFP transgenic mouse brain were isolated by flotation through a sucrose step gradient. The high-speed supernatant (S), high-speed pellet (P), 1.5-M and 2.0-M steps of the gradient, as well as the 0.6- to 1.5-M interface containing the vesicles (V) were blotted with antibodies against Htt, p150^{Glued}, and DIC. (*B*) Vesicles were preincubated with motility assay buffer containing no antibody (yellow), anti-Myc (blue), mouse monoclonal anti-Htt (red), or rat monoclonal anti-Htt (green) and then flowed into a chamber containing microtubules and analyzed by total internal reflection microscopy. Microtubules of similar lengths were analyzed (SEM, $n = 15$ for each condition). (*C*) Vesicle movement was reduced from 62 ± 4% in the presence of control antibody (SEM, $n = 30$) to 23 ± 7% in the presence of mouse monoclonal anti-Htt (SEM, $n = 22$). Stationary vesicles increased from 38 ± 4% in the presence of control antibody to 77 ± 7% in the presence of mouse monoclonal anti-Htt. (*D*) Inhibition of vesicle motility was bidirectional in assays repeated with polarity-marked microtubules. In the presence of mouse monoclonal anti-Htt, vesicle motility in both the minus-end and plus-end directions was reduced. (*E*) Dynein is not lost from vesicles in the presence of anti-Htt antibodies. Vesicles isolated as in *A* were preincubated with antibodies and then laser-bleached to quench the fluorescent signal of the p50-GFP; the number of bleaching events required to completely quench each vesicle was recorded. There were no significant differences between vesicles preincubated with no antibody ($n = 50$) (yellow), anti-Myc control antibody ($n = 61$) (blue), or mouse monoclonal anti-Htt ($n = 68$) (red). Vesicles requiring >20 bleach events were considered aggregates and excluded from further analysis. (*Inset*) Vesicles were preincubated with antibodies and then centrifuged at high speed. Pellets from vesicles preincubated with no antibody (no Ab), mouse monoclonal anti-Htt (ms-Htt), rat monoclonal anti-Htt (rt-Htt), or anti-Myc antibodies were blotted for DIC and actin (as a loading control).

along the microtubules by Htt antibodies suggests that Htt facilitates bidirectional vesicle motility.

To test whether the anti-Htt antibodies decreased the amount of dynein associated with membranes, the vesicles were pelleted after incubation with antibodies. No loss of dynein (Fig. 4*E Inset*) or dynactin (data not shown) was observed from vesicles incubated with anti-Htt antibodies. We also analyzed the association of dynein/dynactin with vesicles by using quantitative bleaching experiments (Fig. 4*E*), but saw no significant decrease in the mean number of bleaches per vesicle induced by the Htt antibody compared with anti-Myc (7.9 ± 0.4 vs. 8.0 ± 0.5). The observed inhibition by the Htt antibodies may be explained by a steric interference imposed on the motors that are in close proximity to the Htt epitope. Htt antibodies may lock the dynein into place on the vesicles because there was actually a 1.5-fold increase in dynein in the vesicles that have been treated with Htt antibodies (Fig. 4*E Inset*). This slight trend toward more dynein on Htt antibody-treated vesicles, although statistically insignificant, is also reflected in the bleaching data because the mode (the number of bleaching events that most vesicles required for quenching) increased from six in the presence of Myc antibody to nine in the presence of Htt antibody (Fig. 4*E*).

Taken together, these results indicate that DIC and Htt associate in cells, and this interaction facilitates dynein-mediated vesicular transport. To further establish a functional relationship between dynein and Htt *in vivo*, we immunostained the dynein RNAi cells for Htt (Fig. 5*A*). A significant portion of Htt-labeled structures were redistributed to the outer cortex in the cells, indicating that trafficking of Htt toward the cell center depends on dynein-based transport. Likewise, in HeLa cells overexpressing p50-GFP, which inhibits the dynein/dynactin complex, Htt was also visible on the cell periphery, as opposed to its concentration at the cell center in nontransfected cells (Fig. 5*B*). To determine whether these structures were associating with the cytoskeleton, we stained dynein RNAi cells for microtubules and F-actin (Fig. 5*C*). Both microtubules and actin stress fibers localize to the cortical sites of Htt accumulation. Thus, Htt requires functional dynein to undergo efficient transport from the cell periphery toward the cell center.

Discussion

To date, there are several examples of adaptor molecules recruiting dynein machinery to vesicles (reviewed in ref. 1). Our study identifies a dynein cargo-recruitment paradigm: Htt facilitates dynein/dynactin-mediated vesicular transport through a direct protein–protein interaction between Htt and dynein. Furthermore, we observe that a functional dynein/dynactin complex is responsible for proper localization of Htt in the cell.

Htt has previously been shown to be associated with vesicles in neurons (2) and endocytic vesicles (22). Htt interacts with HAP1, which binds to dynactin (12, 13). Our finding that Htt also binds to dynein supports the model of Htt as a scaffold that brings together vesicle-associated proteins and dynein machin-

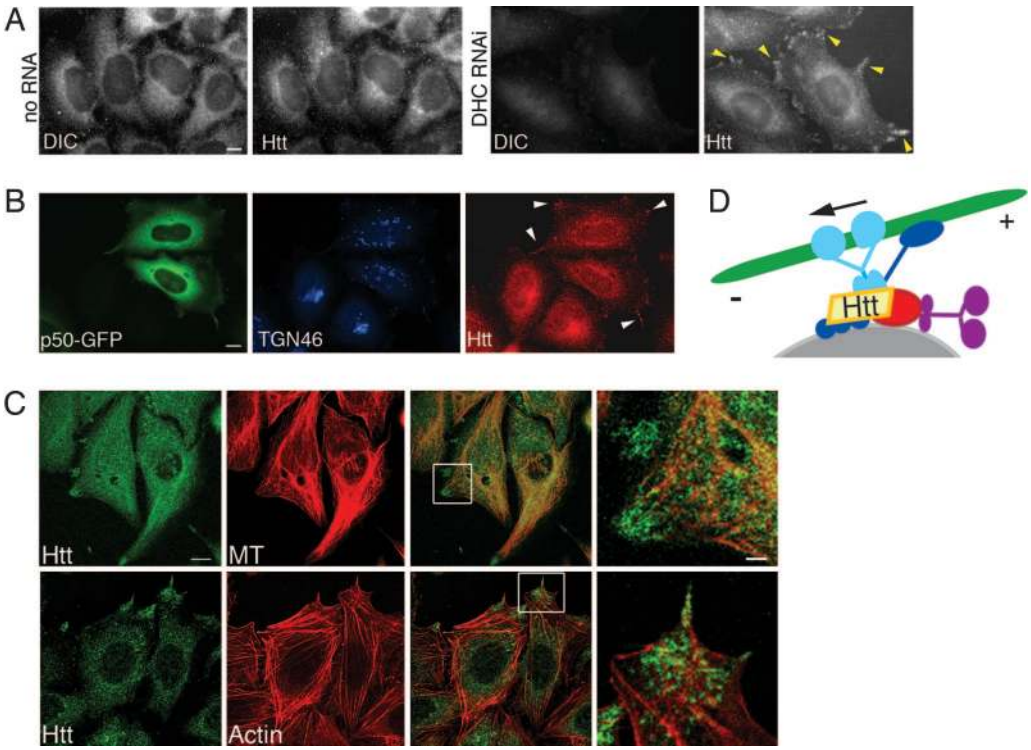

Fig. 5. Htt localization depends on functional dynein. (*A*) (*Left*) No RNA control cells immunostained for DIC and Htt as noted. (*Right*) DHC RNAi cells lack DIC, and Htt is redistributed to the periphery of cells (yellow arrowheads). (Scale bar: 10 μm.) (*B*) HeLa cells transfected with p50-GFP (green) have a disrupted Golgi (TGN46, blue), and Htt (red) is redistributed to the periphery of cells (white arrowheads). (Scale bar: 10 μm.) (*C*) Cortical Htt in DHC RNAi cells overlaps with microtubules (MT) (*Upper*) and F-actin (*Lower*). (Scale bar: 12 μm.) The boxed regions in the merged images are shown at a higher magnification in the far right panel. (Scale bar: 3 μm.) (*D*) Htt is at the center of a multipartite complex facilitating vesicle (gray) recruitment to microtubule motors involving dynein (light blue), dynactin (dark blue), Htt (yellow), HAP1 (red), and kinesin (purple). Arrow denotes direction of movement along microtubule (green).

ery. The DIC-binding site on Htt is between residues 600 and 698, falling between two of the three characterized HEAT (Htt, elongation factor 3, a subunit of protein phophatase 2A, and TOR1) repeat domains. HEAT repeats are highly conserved in Htt, and several Htt HEAT repeat-binding proteins, such as HIP1, HAP1, and HIP14, are involved in trafficking (6). HAP1 has been shown to interact with kinesin (14); in the absence of functional dynein, accumulations of Htt at the cell periphery that we noted are likely due to kinesin-mediated motility. This observation is consistent with the bidirectional block in motility observed *in vitro* when vesicles were treated with anti-Htt antibody. Thus, Htt/HAP1 may act as a docking platform to modulate vesicular cargo attachment to both dynein/dynactin and kinesin microtubule motors.

In our study, cells depleted of Htt by RNAi survived for at least 72 h, consistent with past studies analyzing the survival of individual Htt null cells in chimeric mice and in culture, suggesting that Htt is dispensable for some cell types (23). However, because inactivation of the mouse Htt gene results in embryonic lethality (6), clearly Htt is essential for development of the intact organism, as is dynein (24). Our finding that Htt facilitates dynein-based vesicle motility supports a role for Htt in the dynamic process of vesicle transport during early embryonic development.

We favor a model of Htt as a key factor in promoting association of vesicles with the cytoskeleton. Htt colocalizes with clathrin-coated pits and vesicles at the plasma membrane (22) and may modulate the binding of endocytic vesicles to actin (6). Also, it has recently been proposed that Htt-associated vesicles execute a switch in affinity for specific cytoskeletal filaments based on Htt-binding partners (25). This concept is consistent with our observation that Htt is redistributed to actin-enriched areas of the cell periphery in dynein-depleted cells, indicating that Htt may be associating with actin in the absence of functional dynein. Optineurin, a tether for myosin VI on Golgi membranes, has been proposed to coordinate the activity of actin and microtubule motors based on the finding that optineurin binds to Htt (26). Our finding that Htt interacts directly with dynein provides further evidence for the role of Htt as an integrator of molecular motors and adaptor molecules that can affect a switch in cytoskeletal filament affinity, thus playing a critical role in cytoplasmic vesicle motility.

Huntington's disease is molecularly characterized by the expansion of the polyglutamine tract of the Htt protein. It remains unclear whether the cause of the disease pathology is due to a toxic gain of function and/or loss of normal function. In order to determine whether mutation of Htt results in a loss of normal protein function and, in turn, whether Htt dysfunction contributes to Huntington's disease pathology, the function of Htt must be defined. This study provides insights into the function of Htt in dynein-mediated vesicular transport. Future studies will focus on how mutant Htt may affect dynein-mediated vesicle motility.

Materials and Methods

Yeast Two-Hybrid, Affinity Chromatography, and Immunoprecipitation. Yeast two-hybrid screen and binding tests for proteins interacting with DIC were conducted as previously reported (27, 28); for details see *SI Materials and Methods*. For GST fusion protein experiments, $Htt^{536-698}$ was subcloned into pGEX-6P2 (GE Healthcare, Chalfont St. Giles, U.K.), and interacting proteins were isolated by affinity chromatography with glutathione Sepharose beads. Htt truncation constructs (a gift of M. Zerial, Max-Planck-Institute, Dresden, Germany) were translated *in vitro*, loaded onto DIC affinity columns, washed, and

eluted with 2 M NaCl. For immunoprecipitation, protein A agarose beads were charged with anti-DIC rabbit polyclonal antibody UP1467 (generated in our laboratory) or anti-GFP mouse monoclonal antibody (Clontech, Mountain View, CA), incubated with mouse brain cytosol, washed extensively, and eluted in SDS gel sample buffer.

Transfections and Cell Culture. For RNAi and immunocytochemistry methods, see *SI Materials and Methods*. HeLa-M cells (a gift from A. Peden, Cambridge Institute for Medical Research, Cambridge, U.K.) were transiently transfected with GFP-p50 plasmid DNA (20) by using FuGene (Roche Diagnostics, Indianapolis, IN).

Dynein and Vesicle Purification. Dynein was purified from bovine brain followed by FPLC purification on a Mono Q 10/10 anion exchange column (GE Healthcare) (15). Cytosol was prepared from brains of either wild-type or p50-GFP transgenic mice (20, 29). The 100,000 $\times$ *g* supernatant was used in affinity chromatography assays. The 100,000 $\times$ *g* pellet was fractionated by flotation through a sucrose step gradient with steps of 0.6, 1.5, and 2.0 M sucrose in 0.5$\times$ cell motility buffer as described (29). Vesicles were isolated from the 0.6- to 1.5-M interface.

***In Vitro* Motility Assay and Pelleting.** Vesicles were preincubated with motility assay buffer [10 mM Na-Pipes, 50 mM K-acetate, 4 mM $MgSo_4$, 1 mM EGTA (pH 7.0)] containing either anti-Htt mouse monoclonal antibody MAB2166 (Chemicon International, Temecula, CA), anti-Htt rat monoclonal antibody MAB2174 (Chemicon), or anti-Myc mouse monoclonal antibody (Clontech) for 20 min at 23°C. Samples were then flowed into chambers containing taxol-stabilized rhodamine or polarity-marked microtubules. Vesicular motility (defined as >300 nm excursions along the microtubule) was visualized by using total internal reflection microscopy (20). For pelleting assays, vesicles were preincubated with antibodies as above and then centrifuged at 100,000 $\times$ *g* for 10 min at 22°C. For photobleaching methods, see *SI Materials and Methods*.

This work was supported by National Institutes of Health Grant GM48661.

1. Caviston JP, Holzbaur EL (2006) *Trends Cell Biol* 16:530–537.
2. DiFiglia M, Sapp E, Chase K, Schwarz C, Meloni A, Young C, Martin E, Vonsattel JP, Carraway R, Reeves SA (1995) *Neuron* 14:1075–1081.
3. Gutekunst CA, Levey AI, Heilman CJ, Whaley WL, Yi H, Nash NR, Rees HD, Madden JJ, Hersch SM (1995) *Proc Natl Acad Sci USA* 92:8710–8714.
4. Hoffner G, Kahlem P, Djian P (2002) *J Cell Sci* 115:941–948.
5. Block-Galarza J, Chase KO, Sapp E, Vaughn KT, Vallee RB, DiFiglia M, Aronin N (1997) *NeuroReport* 8:2247–2251.
6. Harjes P, Wanker EE (2003) *Trends Biochem Sci* 28:425–433.
7. Szebenyi G, Morfini GA, Babcock A, Gould M, Selkoe K, Stenoien DL, Young M, Faber PW, MacDonald ME, McPhaul MJ, Brady ST (2003) *Neuron* 40:41–52.
8. Gunawardena S, Her LS, Brusch RG, Laymon RA, Niesman IR, Gordesky-Gold B, Sintasath L, Bonini NM, Goldstein LS (2003) *Neuron* 40:25–40.
9. Trushina E, Dyer RB, Badger JD, Ure D, Eide L, Tran DD, Vrieze BT, Legendre-Guillemin V, McPherson PS, Mandavilli BS (2004) *Mol Cell Biol* 24:8195–8209.
10. Gauthier LR, Charrin BC, Borrell-Pagès M, Dompierre JP, Rangone H, Cordelières FP, De Mey J, MacDonald ME, Lessmann V, Humbert S, Saudou F (2004) *Cell* 118:127–138.
11. Li SH, Li XJ (2004) *Trends Genet* 20:146–154.
12. Engelender S, Sharp AH, Colomer V, Tokito MK, Lanahan A, Worley P, Holzbaur EL, Ross CA (1997) *Hum Mol Genet* 6:2205–2212.
13. Li SH, Gutekunst CA, Hersch SM, Li XJ (1998) *J Neurosci* 18:1261–1269.
14. McGuire JR, Rong J, Li SH, Li XJ (2006) *J Biol Chem* 281:3552–3559.
15. Bingham JB, King SJ, Schroer TA (1998) *Methods Enzymol* 298:171–184.
16. Burkhardt JK, Echeverri CJ, Nilsson T, Vallee RB (1997) *J Cell Biol* 139:469–484.
17. Echeverri CJ, Paschal BM, Vaughan KT, Vallee RB (1996) *J Cell Biol* 132:617–633.
18. He Y, Francis F, Myers KA, Yu W, Black MM, Baas PW (2005) *J Cell Biol* 168:697–703.
19. Levy JR, Sumner CJ, Caviston JP, Tokito MK, Ranganathan S, Ligon LA, Wallace KE, LaMonte BH, Harmison GG, Puls I, *et al.* (2006) *J Cell Biol* 172:733–745.
20. Ross JL, Wallace K, Shuman H, Goldman YE, Holzbaur EL (2006) *Nat Cell Biol* 8:562–570.
21. Waterman-Storer CM, Karki SB, Kuznetsov SA, Tabb JS, Weiss DG, Langford GM, Holzbaur EL (1997) *Proc Natl Acad Sci USA* 94:12180–12185.
22. Velier J, Kim M, Schwarz C, Kim TW, Sapp E, Chase K, Aronin N, DiFiglia M (1998) *Exp Neurol* 152:34–40.
23. Reiner A, Dragatsis I, Zeitlin S, Goldowitz D (2003) *Mol Neurobiol* 28:259–276.
24. Harada A, Takei Y, Kanai Y, Tanaka Y, Nonaka S, Hirokawa N (1998) *J Cell Biol* 141:51–59.
25. Pal A, Severin F, Lommer B, Shevchenko A, Zerial M (2006) *J Cell Biol* 172:605–618.
26. Sahlender DA, Roberts RC, Arden SD, Spudich G, Taylor MJ, Luzio JP, Kendrick-Jones J, Buss F (2005) *J Cell Biol* 169:285–295.
27. Ligon LA, Tokito M, Finklestein JM, Grossman FE, Holzbaur EL (2004) *J Biol Chem* 279:19201–19208.
28. Wagner OI, Ascaño J, Tokito M, Leterrier JF, Janmey PA, Holzbaur EL (2004) *Mol Biol Cell* 15:5092–5100.
29. Holleran EA, Ligon LA, Tokito M, Stankewich MC, Morrow JS, Holzbaur EL (2001) *J Biol Chem* 276:36598–36605.